Thermomechanical Characterization of Thermoset Urethane Shape-Memory Polymer Foams

Linda Domeier, April Nissen, Steven Goods, LeRoy Whinnery, James McElhanon

Sandia National Laboratories, Livermore, California 94550

Received 7 July 2009; accepted 4 September 2009
DOI 10.1002/app.31413
Published online 3 November 2009 in Wiley InterScience (www.interscience.wiley.com).

ABSTRACT: The shape-memory polymer performance of urethane foams compressed under a variety of conditions was characterized. The foams were water-blown thermosets with a closed-cell structure and ranged in density from about 0.25 to 0.75 g/cm^3. Compressive deformations were carried out over a range of strain levels, temperatures, and lateral constraints. Recovery stresses measured between fixed platens were as high as 4 MPa. Recovery strains, measured against loads up to 0.13 MPa, demonstrated the effects of various parameters. The results suggest that compression near the foam glass-transition temperature provided optimal performance. Foams with densities of about 0.5 g/cc and compressed 50% provided a useful balance (time, strain, and load) in the recovery performance. © 2009 Wiley Periodicals, Inc.† J Appl Polym Sci 115: 3217–3229, 2010

Key words: macroporous polymers; mechanical properties; polyurethanes; stimuli-sensitive polymers; thermosets

INTRODUCTION

Shape-memory polymers (SMPs) are materials that can be deformed, usually in the rubbery state at an elevated temperature, cooled in that new shape to a glassy state that preserves the deformation, and later reheated to the rubbery state where they entropically recover their original shape. In contrast to shape-memory alloys and ceramics, SMPs can be deformed over a wider range of designed temperatures and to much larger strains, depending on the polymeric material. The variety of polymeric types capable of displaying useful SMP behavior range from high-molecular-weight thermoplastics with entangled networks to covalently crosslinked thermosets to thermoplastics with crystallizable domains and others. Almost all polymers can exhibit some level of shape-memory behavior under the appropriate conditions.

Commercial SMP applications, such as heat-shrink films and tubing, are well known, and the complex science behind these materials continues to be studied.[1,2] Newer medical and engineering applications, exemplified by the increasing numbers of patents and literature reports, are being pursued with urethanes, epoxies, acrylics, and biodegradable polymers.[3–8] Specific urethane laminates have enabled the fabrication of a two-way shape-memory system.[9] Several reviews of the field have been published,[10–14] and a variety of constitutive models of SMP materials have also been developed.[15–19]

Optimizing the design of SMP actuated devices requires an understanding of the work available from the SMP material, the amount of recovery force that can be generated, and the rate and extent of strain recovery. Both recovery strain and stress performance depend on the polymer composition and form (film, foam, laminate, etc.), the sample geometry, the processing history of the material, its heat-transfer properties, and the deformation, storage, and activation conditions. The recoverable stress and strain can only be as large as the deformation stress and strain, whereas the stress relaxation and creep during deformation, storage, and recovery can all decrease performance. Many of these interactions have only begun to be explored in depth but clearly demonstrate the ability to manipulate SMP performance through adjustments to the deformation parameters.[5,20,21]

Most materials must be in a nonglassy state to allow deformation without permanent damage to the polymeric structure. The transition from the glassy to the rubbery state takes place over a temperature range, however, and deformation at a temperature within that range where the modulus has not fully decreased to the rubbery level requires a higher deformation stress and offers a potentially higher recovery stress. Studies on samples deformed in a bending mode have demonstrated such enhanced recovery peak stresses when deformation was carried out at lower temperatures.[5,20]

Correspondence to: L. Domeier (ladomei@sandia.gov).

Deformation within the glass-transition temperature (T_g) region has also been shown to allow higher tensile strain to failure values than deformations in either the glassy or rubbery state.[21]

Recovery performance during the heating of an SMP can be characterized by measurement of the recovery strain with no imposed stresses on the sample (free recovery), measurement of the recovery stress while the sample strain is fixed, and measurement of the recovery strain against a range of imposed stresses.[22] The latter approach provides useful design parameters for foams and other SMP actuators and presents a situation intermediate to fully constrained and unconstrained recovery.

The expansion of compressed SMP foams is a simple actuation process, which has been explored in a limited number of low-density foam systems.[22–27] Most of these studies[22,24–27] evaluated proprietary foams obtained as slab stock from Mitsubishi Heavy Industries, primarily Mitsubishi MF5520 with limited work on MF21.[25] The foams were described as open-cell, thermoplastic polyurethanes with reported T_g values in the 40–65°C range. Because of their relatively low T_g values, some compressed samples required constrained storage[22] to prevent gradual reexpansion at room temperature. MF5520 has a reported density of 0.032 g/cm,[3,7] whereas MF21 has a reported expansion ratio of 30,[25] which suggests a similarly low density. Compressions were carried out with no lateral constraints.

The low densities and open-cell structure of these foams allow facile compression to high strain levels but also result in relatively low recovery stresses. They are most suited for applications that allow free strain recovery. Samples compressed to 80–90% showed almost complete strain recovery upon reheating to or above the T_g.[24–27] Compression deformation stresses varied as expected with temperature, strain, and strain rate but were all less than 200 kPa. Subsequent recovery stresses varied further with storage conditions.

A commercial thermoset epoxy foam ($T_g \approx 90$°C, density = 0.2 g/cm^3) from Composite Technology Development was also evaluated.[23] The foam contained a mixture of open- and closed-cell structures with a high percentage of closed cells. A range of compressive and tensile characterizations were carried out both above and below T_g. The SMP compressive deformation and recovery cycles showed higher recovery stresses, about 120 kPa, in foams deformed at 100°C than in those deformed at 125°C, both to 80% strain, which was maintained during the stress-recovery measurements. Free strain recoveries were over 90% in both cases.

In addition to the Mitsubishi SMP foams, thermomechanical characterizations of a range of solid Mitsubishi thermoplastic urethane SMPs were carried out with either cast- or melt-processed samples.[4] It is not known if any of these had compositions similar to the Mitsubishi foams discussed previously. The effects of the processing and thermal history on the sample mechanical performance were evident. Tensile stress values above T_g were approximately 10 MPa at 100% elongation in these unfoamed materials. Other tensile studies on the Mitsubishi urethane SMPs clearly demonstrated the loss of recovered strain when the samples were stored at or above T_g.[28,29]

In other work, urethane SMPs with uniform aliphatic networks, designed to provide a sharp T_g transition, were prepared, characterized, and shown to have tensile moduli in the 25-MPa range, above those seen with the Mitsubishi systems, although elongation was limited to about 35%.[30] Polycaprolactone-based urethanes with a range of compositions were synthesized to evaluate the effects of the composition on the SMP behavior and demonstrated recovery stresses up to 6 MPa in film tensile tests at a fixed strain.[31] Urethane films with various butane diol based hard segments showed increasing recovery stresses with increasing hard segment content and also showed higher stresses, attributed to higher orientation effects, when they were fabricated into fibers.[32] At 50% strain, the films had stresses of about 3 MPa, and the fibers had stresses of about 6 MPa.

None of these studies evaluated higher density foams or systematically characterized the effects of the foam density and deformation parameters on the SMP recovery behavior. An additional and unexplored deformation parameter available with foam samples is the lateral constraint on the materials during compression. Both of these parameters, higher foam density and the lateral compression constraint, were explored here along with other parameters discussed later.

The foams characterized in this study were originally developed at Sandia National Laboratories for their enhanced toughness and crack resistance during impact. They were rigid, closed-cell, water-blown polyurethane foams that generated carbon dioxide during the foaming and curing process and could be readily formulated to provide a range of densities. Closed-cell foams are generally more difficult to deform in the rubbery state than open-cell foams and are expected to provide stronger recovery stresses as a result. Early SMP evaluations of these foams found excellent strain recovery, and the unfoamed solid polymer also showed good performance in a slightly isocyanate-rich formulation.

To provide actuator design guidance, a more extensive characterization of the SMP recovery behavior of these materials was carried out. Foams with relatively high densities of about 0.25, 0.50, and 0.75 g/cm^3 were prepared and machined into

appropriate test specimens. T_g transitions of the foams and solids were characterized by dynamic mechanical analysis (DMA) measurements of the moduli during heating and cooling scans.

Test frame measurements of the compressive stress–strain behavior were carried out on cylindrical samples at different temperatures and strains. We measured the recovery stresses by heating the compressed samples between fixed platens.

The cylindrical samples used in the DMA recovery tests were compressed, unless beyond the compression limits of the sample, to strains of 25, 50, and 75% at temperatures ranging from about 20°C above to 20°C below the T_g value (110–150°C). During compression, the foam samples were laterally constrained to different diameters; in some cases, this allowed free expansion in the lateral plane. The cooling rate was rapid for most samples except for a limited number of comparisons with a slower cooling rate. Recovery profiles of the compressed samples were measured against a range of imposed stresses.

EXPERIMENTAL

Foam formulation, processing, and sample fabrication

The polyether polyol, surfactant, and water were mixed by hand. A catalyst was then added with further hand mixing followed by the diisocyanate and 45 s of mixing with a Conn blade (IT, intensive type). The resin mixture was poured into cylindrical steel molds (7.6 cm high × 7.8 cm in diameter) with vented tops (a distribution of small holes), cured at room temperature for about 4 h, cured overnight at 65°C, and allowed to cool. We removed the foam cylinders, cut them in half to get two shorter cylinders, and then postcured them by heating them to 150°C at 2°C/min, holding them at 150°C for 120 min, and then cooling them at 2°C/min to 60°C before removing them from the oven.

One surface of each cylindrical block was machined off to provide a fresh, skin-free surface. Small cylindrical samples were then bored into each block with a machine drill press and appropriate diameter rotary dies. The boring depth did not penetrate the entire block, which left the small cylinders embedded at their base in the original block. The entire block was then cut with a band saw into thinner 10.2-mm (0.4-in.) slices, from which the unattached test sample cylinders could be removed. Small machining defects were removed by hand with a file. The same machining techniques were used to fabricate larger samples for the test frame experiments.

Compression experiments (DMA samples)

Foam cylinders 10.2 mm (0.4 in.) in height and 12.7 mm (0.5 in.) in diameter were placed in lubricated (Teflon spray) cylindrical cavities with a diameter of 12.7, 15.2, or 17.8 mm (0.5, 0.6, or 0.7 in.) in an aluminum block 38 mm in height. Aluminum cylinders 38 mm high and slightly smaller than the cavity diameters were placed on top of the foam cylinders. Steel spacers with a height that allowed the aluminum cylinders to compress the foam samples to a final height of 2.5, 5.1, or 7.6 mm (0.1, 0.2, or 0.3 in.) were arranged on the surface of the aluminum block. The entire assembly was placed in a Carver Model 3925 hydraulic press (Wabash, IN), and the platens were closed to just make contact with the protruding aluminum cylinders. The press platens were heated to the deformation temperature and held at that temperature for 30 min to ensure equilibration throughout the foam samples. The platens were then closed to the height defined by the aluminum block and steel spacers by hand pumping over a period of about 30 s. Cooling water was immediately circulated to bring the platens to 40°C over a period of about 10 min. The bottom platen was then lowered, and the aluminum block assembly was removed. After complete cooling to room temperature, the foam cylinders were removed from the cavities. In a limited number of experiments, the platens were allowed to cool passively with no cooling water and took approximately 180 min to reach 70°C.

DMA evaluations

Dynamic mechanical analyses were carried out on a TA Instruments (New Castle, DE) Q800 DMA.

T_g's were determined from modulus–temperature scans in a dual-cantilever clamp with rectangles ($35 \times 10 \times 2.5$ mm^3) cut from the same foam blocks as the cylindrical samples. The samples were heated at 3°C/min to 160°C, and the T_g values were determined for the onset, midpoint, and end of the storage modulus decrease.

Measurements of the recovery strain of the compressed foam cylinders were made with the compression clamp in the controlled force mode over a range of imposed preload forces. The samples were equilibrated for 10 min at 60°C, then heated to 160°C at a rate of 5°C/min, and held at 160°C for 30 min. The rate and extent of the recovery strain were measured.

Test frame compression and recovery evaluations

Test frame measurements were made on a Satec 22 EMP electromechanical test frame equipped with a noncontacting laser extensometer (Electronic

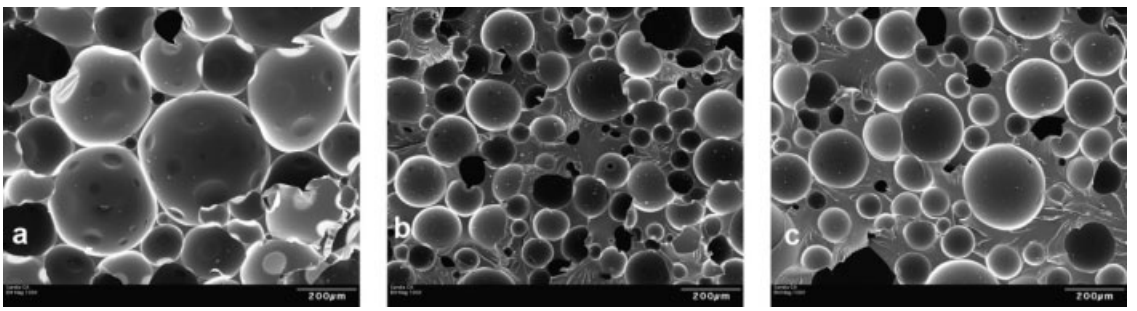

Figure 1 Scanning electron microscopy images of the fracture surface of (a) 0.25, (b) 0.50, and (c) 0.75 g/cc foams.

Instruments Research, Irwin, PA, model LE-01) to measure displacements. The 25.4 × 25.4 mm^2 foam cylinders were inserted in a steel die to provide lateral constraint during the initial compression. The samples in the die were slowly brought to temperature in an environmental test chamber and equilibrated for 1 h before compression. All specimens were compressed to a final density of approximately 0.9 g/cc (or about 80% of the maximum theoretical density of the solid polymer).

To increase the thermal response of the test apparatus for the recovery measurement, the compressed specimens were transferred to a thin-walled aluminum die that was wrapped with heating tape. This allowed for a reheating rate of approximately 4–5°C/min. Upon heating, the compressed cylinders expanded against the fixed load train of the test frame, and the recovery stresses or pressures were measured up to 160°C.

RESULTS AND DISCUSSION

The closed-cell nature of these urethane foams is shown in Figure 1 in a series of scanning electron microscopy images representative of the three densities of foam used in this study. The surfaces shown are the result of a fracture driven by the bending of 1 × 1 × 5-cm^3 samples of the foams. In each of the images, the inside of the cells are shown with fractures in the solid polyurethane that comprised the matrix. In the low-density image [Fig. 1(a)], windows are shown within the cells where neighboring cells met. In the two higher density foams [Fig. 1(b,c)], very few of these windows are shown because of the greater amount of solid polymer available to fill between the cells. As is common in blown foams, the lower density foam had a larger average cell size.

The SMP foam parameters evaluated in the study are shown in Table I. A separate test series evaluated the effects of the foam cylinder diameter. For the parameter evaluations shown in Table I, the size of the cylinders used in the test frame compressions and recoveries was fixed at 25.4 mm high × 25.4 mm in diameter, and the cylinders used in the DMA recovery tests were fixed at 10.2 mm high × 12.7 mm in diameter.

Not all of the possible parameter combinations could be evaluated (because of compression limits as foam density increased), and others were not evaluated as they were judged unnecessary. Approximately 150 different combinations were tested, the majority at 50% compression with smaller numbers at 25 and 75% compression.

As shown in Table II, decreasing foam density led to slightly higher T_g values because of the increased formation of urea linkages with higher water content. Onset T_g values were generally about 130°C for the range of densities studied, and the midpoint T_g values were generally about 140°C.

The initial study on the effect of the foam diameter on recovery used lower density foams about 0.1 g/cc in density. Cylinders 10.2 mm high and with diameters ranging from 5 to 14 mm were compressed 30% at 160°C, and the recovery strain was measured by DMA under minimum contact

TABLE I
Foam Material and Processing Parameters

Foam density	~ 0.25, 0.50, and 0.75 g/cc
Compression temperature	~ 110, 120, 130, 140, and 150°C
Compression strain	~ 25, 50, and 75%
Lateral constraint during compression	Cylinder diameters × 1.0, 1.2, and 1.4
Cooling rate	Active (fast) versus passive (slow)
Foam cylinder diameter	Separate series with diameters from 5 to 14 mm
Pressure during recovery	Contact, 0.05, 0.10, and 0.13 MPa

TABLE II
T_g Values Determined from the Storage Modulus Curves (Initial Heating Cycle)

Foam density	Onset	Midpoint	End
0.25 g/cc	134°C	142°C	148°C
0.50 g/cc	131°C	139°C	146°C
0.75 g/cc	131°C	138°C	145°C

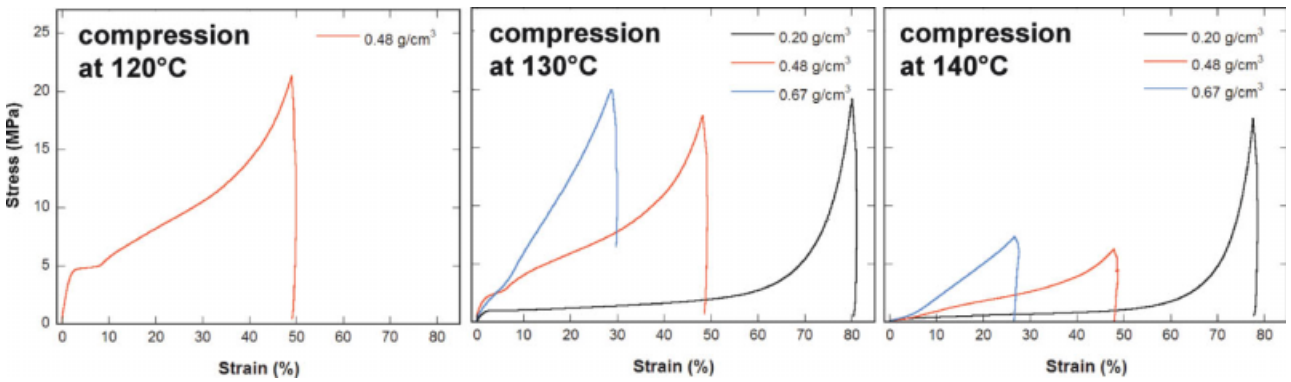

Figure 2 Compression stress and relaxation for the foam cylinders compressed at 120–140°C. [Color figure can be viewed in the online issue, which is available at www.interscience.wiley.com.]

pressure. One series of samples was heated at 3°C/min and another was heated at 10°C/min to 160°C and that temperature was then maintained until recovery was complete. No consistent correlation of the recovery time with the foam cylinder diameter was noted in either series, and the samples heated at 10°C/min actually showed slightly faster recoveries for the larger diameter cylinders. Similar measurements were not made on the higher density foams used in this study, and the foam cylinder diameter was instead fixed as noted previously.

Test frame measurements of the compressive and recovery stresses

Compressive stresses were measured at 130 and 140°C for three foam densities and at 120°C for one density, as shown in Figure 2. The compressive stress levels, as expected, decreased with increasing temperature. Different density foams were compressed to different final strains, each representing about 80% of the maximum density. At the same strain level, higher density foams, again as expected, showed higher stress values. The highest compressive stress values noted were in the range 7–20 MPa. As was clear from the plots, the stress relaxation after compression was extremely rapid. The cooling rates were about 2°C/min, and the foam samples eventually lost contact with the platen because of thermal shrinkage.

After cooling and fixing the platen 0.5 mm above the plunger on top of the compressed foam samples, we measured the recovery stresses at a heating rate of 3–5°C/min. The samples were contained in aluminum cylinders, as described in the Experimental section. The effect of the foam density on the recovery stress is shown in Figure 3 and Table III. Higher density foams provided higher recovery stresses. Lower compression temperatures also raised the peak stresses. The highest recovery stress, 4 MPa,

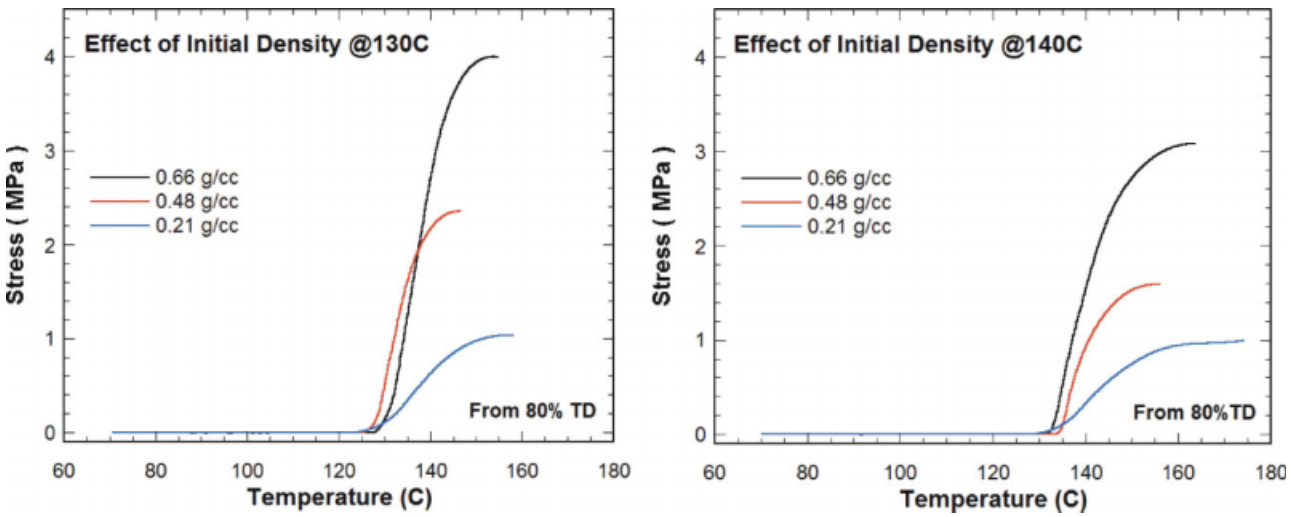

Figure 3 Recovery stress measurements for foam cylinders compressed at 130 and 140°C, cooled, and then reheated. From 80% TD, indicates that foams had been compressed to 80% of the theoretical maximum density. [Color figure can be viewed in the online issue, which is available at www.interscience.wiley.com.]

TABLE III
Peak Recovery Stresses in the Foam Cylinders (Initial Reheating)

	Peak recovery stress (MPa)		
Foam density	0.20 g/cc	0.48 g/cc	0.67 g/cc
Compression strain	78%	48%	27%
Compressed at 120°C		2.4	
Compressed at 130°C	1.0	2.3	4.0
Compressed at 140°C	0.9	1.6	3.1

was measured in a 0.67 g/cc foam compressed 27% at 130°C. All of the samples showed peak recovery stresses of about 1 MPa or higher.

Little correlation was noted between the maximum compressive stress and the recovery stress because of the rapid relaxation of the compression stress, evident in the Figure 2 plots. In DMA strain recoveries discussed later, different cooling rates had only minor effects on SMP recovery. Both results reflect the need for almost instantaneous cooling to prevent this rapid initial relaxation.

The effects of the compression temperature were evaluated at 120, 130, and 140°C with the 0.48 g/cc foam. As shown in Table III and Figure 4, little additional increase in the peak recovery stress was noted in this single trial at 140°C. The onset of recovery, however, was shifted to lower temperatures as the compression temperature was reduced from 140 to 130 to 120°C, and similar effects were seen in the recovery strain experiments discussed later.

The effects of repeated SMP cycles were evaluated with a single 0.48 g/cc foam sample compressed three times at 120°C, as shown in Figure 5. The peak recovery stress decreased with each cycle, and the onset of recovery was also shifted to lower temperatures. This may have been because of accumulated damage in the foam.

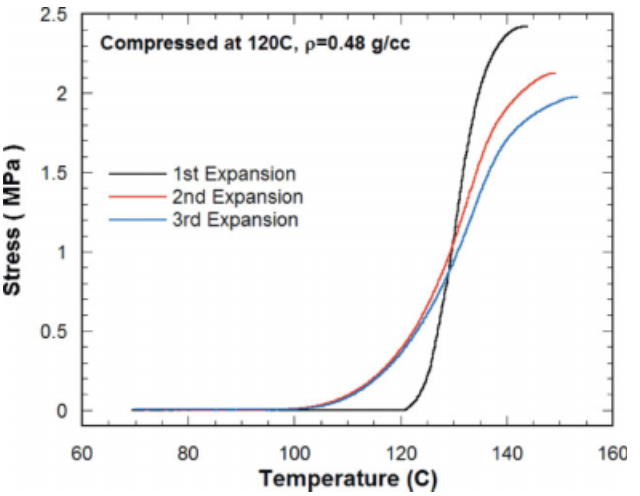

Figure 5 Repeated compression-recovery SMP cycles on the 0.48 g/cc foam compressed at 120°C. [Color figure can be viewed in the online issue, which is available at www.interscience.wiley.com.]

DMA measurements of the recovery strain

Samples used in the DMA recovery experiments were compressed in a Carver press, as described previously. They were then reheated in the DMA in the controlled force mode with the compression clamp, and the strain was measured during the temperature ramp. The temperature ramp was identical for all runs: samples were equilibrated at 60°C, ramped from 60 to 160°C at 5°C/min (20 min total), and held at 160°C for 30 min.

A typical series of strain-recovery runs is shown in Figure 6, including the recompression observed in

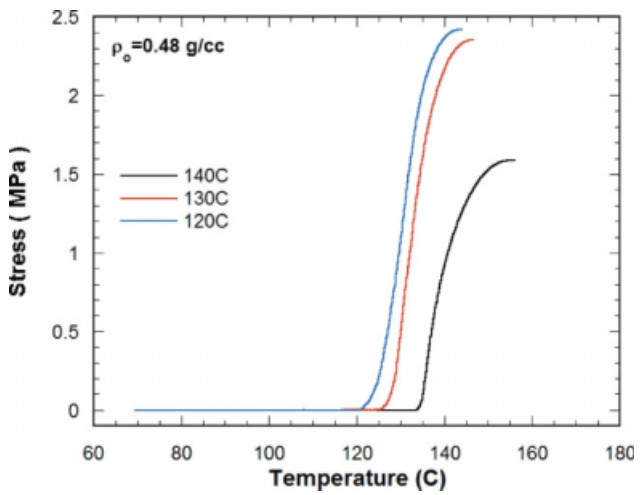

Figure 4 Recovery stresses for the 0.48 g/cc foams compressed at 120, 130, and 140°C. [Color figure can be viewed in the online issue, which is available at www.interscience.wiley.com.]

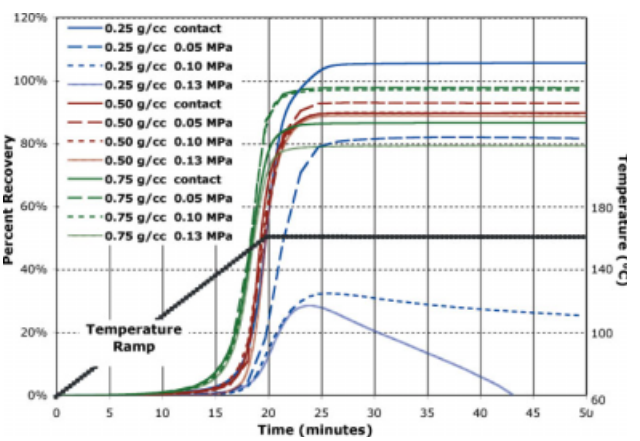

Figure 6 One subset of strain-recovery experiments (three foam densities compressed 50% at 130°C, 0.25/0.50 g/cc foams compressed in 12.7-mm diameter cavities, and 0.75 g/cc foams compressed in 15.2-mm diameter cavities). [Color figure can be viewed in the online issue, which is available at www.interscience.wiley.com.]

DMA Force (MPa)	Foam Density (g/cc)	Compr. Temp (°C)	Constraint Diameter (inches)	Percent Compression
0.00	0.25	120	0.5	25%
0.05	0.50	130	0.6	50%
0.10	0.75	140	0.7	75%
0.13		150		

Figure 7 Color formatting of the recovery data spreadsheets (constraint diameters shown in inches for simplicity). [Color figure can be viewed in the online issue, which is available at www.interscience.wiley.com.]

two low-density foams heated under loads of 0.10 and 0.13 MPa. The temperature ramp is also shown, which reached 160°C in 20 min. All of the foams shown in this figure were compressed to 50% strain at 130°C in cavities with either 12.7 or 15.2 mm diameters. Foams of all three densities are shown in runs with all four DMA compression pressures (contact, 0.05, 0.10, and 0.13 MPa). The complexity and multitude of such plots made the effects of some parameters clear but obscured the overall trends in many cases. Over 150 compressions and strain-recovery experiments were completed.

Extracting the trends from these data was done both with Excel spreadsheets with color-coded conditional formats or with averaged plots of all of the data sorted by single parameters. In both cases, the effects of each parameter on the time to 2, 20, 40, and 60% recovery were examined.

A sample of a formatted spreadsheet is shown in Figure 7, which includes five columns, one each for the DMA pressures (four values), foam densities (three values), compression temperatures from 120 to 150°C (four values with the limited data at 110°C are discussed separately later), lateral constraint diameters (three values), and compression strains (three values). Within each column, different values for that variable are assigned different colors, as shown with the lowest value being white, the next highest blue, then pink, and the highest value yellow. Grouping of the white, blue, pink, or yellow colors in a given column easily indicated where that parameter affected a sorted data set. For example, spreadsheets in which the compression temperature column in the middle had a concentration of white and blue cells near the bottom indicated that lower compression temperatures (120–130°C) resulted in shorter recovery times.

This same formatting was applied to the entire data set when it was sorted by descending times to 2, 20, 40, and 60% recovery, as shown in Figure 8, with slow recoveries at the top and faster recoveries at the bottom. Each spreadsheet for 2, 20, 40, or 60% recovery displayed five columns, formatted as shown in Figure 7. The cells were compressed in height to show all 153 runs.

The red circles in Figure 8 indicate significant groupings of data. The first column, the pressure during the DMA run, ranging from contact to 0.13 MPa,

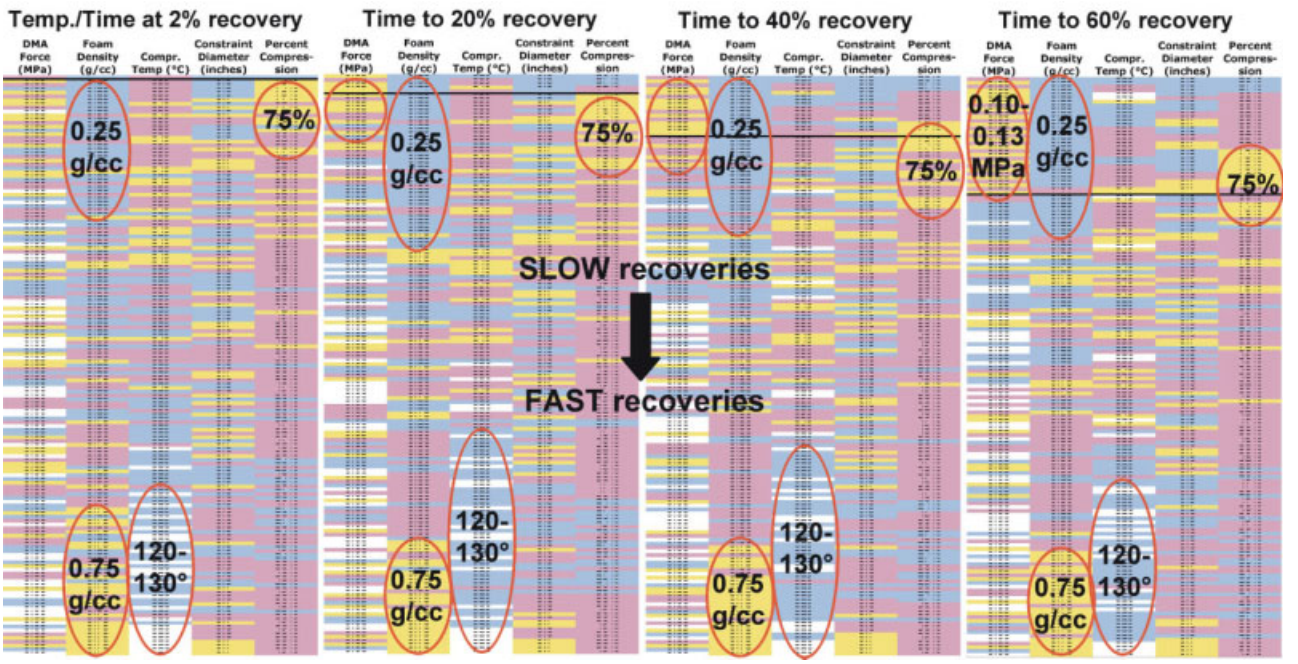

Figure 8 Color-formatted spreadsheets showing samples with different parameters (DMA pressure, foam density, compression temperature, constraint diameter, and percentage compression) ranked in order of recovery time. The recovery time ranges were 22–8 min at 2%, 25–15 min at 20%, 29–17 min at 40% and 34–18 min at 60%. Significant data groups are circled. Samples above the black line in each group did not recover to that percentage level or showed recompression. [Color figure can be viewed in the online issue, which is available at www.interscience.wiley.com.]

clearly was not a dominant factor, except for the lowest density foams. The second column, the foam density, shows faster recovery times for the higher density foams and slower recovery times, or even recompression, for the 0.25 g/cc foams (blue), especially under higher DMA pressures. The third column, the compression temperature, shows faster recoveries when the samples were compressed at lower temperatures (white and blue). This is discussed further later with the inclusion of compressions at 110°C. The fourth column, the lateral constraint diameter during compression, did not have a significant impact on the foam recovery (exceptions are discussed later). The urethane foams in this study did not bulge excessively during free compression, and such lateral constraint may be more significant in other foams. Higher lateral constraints did reduce flaking at the surface of the compressed foam cylinders. The last column, the percentage compression, was a restricted variable, in that only the 0.25 g/cc foams were compressed 75% and those samples often showed slower recoveries. The majority of the compressions were taken to 50% strain (pink) with fewer compressions at 25% (blue) and 75% (yellow).

In Figure 9, we detail one subset of the data in Figure 8, the 60% recovery times, by subdividing

Contact Pressure

Foam Density (g/cc)	Compr. Temp (°C)	Constraint Diameter (inches)	Percent Compression	60% time (min)
0.25	140	0.5	73%	24.1
0.25	140	0.6	75%	22.8
0.25	140	0.5	73%	22.3
0.25	140	0.7	75%	22.3
0.25	150	0.5	50%	21.6
0.50	150	0.7	51%	21.4
0.50	150	0.6	51%	21.4
0.25	140	0.7	51%	21.4
0.25	130	0.5	72%	21.4
0.25	140	0.6	51%	21.2
0.25	140	0.5	49%	21.1
0.75	150	0.6	52%	20.9
0.75	140	0.7	51%	20.8
0.25	130	0.6	75%	20.7
0.25	130	0.6	49%	20.6
0.50	150	0.5	47%	20.5
0.50	140	0.7	50%	20.4
0.50	140	0.6	49%	20.3
0.25	130	0.7	50%	20.3
0.50	140	0.5	48%	20.3
0.25	140	0.5	26%	20.2
0.25	130	0.5	48%	20.1
0.50	130	0.7	51%	19.9
0.25	120	0.6	50%	19.7
0.25	130	0.5	24%	19.7
0.50	120	0.5	45%	19.6
0.50	130	0.5	47%	19.6
0.50	120	0.6	51%	19.6
0.25	120	0.5	48%	19.6
0.50	130	0.6	50%	19.5
0.75	130	0.5	23%	19.4
0.75	130	0.6	27%	19.4
0.75	140	0.6	50%	19.0
0.75	130	0.6	49%	18.9
0.50	130	0.6	26%	18.9
0.75	120	0.6	49%	18.9
0.50	130	0.5	23%	18.5
0.75	130	0.7	49%	18.4
0.75	120	0.7	49%	17.8

0.05 MPa Pressure

Foam Density (g/cc)	Compr. Temp (°C)	Constraint Diameter (inches)	Percent Compression	60% time (min)
0.25	140	0.6	77%	25.9
0.25	140	0.5	74%	25.1
0.25	140	0.5	75%	24.6
0.25	140	0.7	76%	24.6
0.25	140	0.6	52%	24.4
0.25	140	0.5	27%	24.0
0.25	150	0.5	51%	23.9
0.25	140	0.7	52%	23.9
0.50	150	0.7	52%	23.7
0.25	140	0.5	51%	23.3
0.25	130	0.5	75%	22.7
0.25	130	0.6	51%	22.7
0.75	140	0.7	52%	22.6
0.75	150	0.6	51%	22.4
0.50	150	0.6	51%	22.2
0.25	130	0.5	50%	22.1
0.25	130	0.7	51%	22.0
0.25	130	0.5	26%	22.0
0.50	130	0.5	24%	21.5
0.50	140	0.7	51%	21.4
0.25	120	0.5	49%	21.1
0.25	120	0.6	51%	21.1
0.50	140	0.6	51%	21.1
0.50	150	0.5	48%	21.0
0.75	140	0.6	51%	21.0
0.50	140	0.5	46%	20.3
0.50	130	0.6	52%	20.3
0.50	130	0.7	51%	20.2
0.50	120	0.5	47%	20.0
0.50	120	0.6	51%	20.0
0.50	130	0.5	48%	19.9
0.75	130	0.6	27%	19.6
0.75	120	0.6	50%	19.4
0.50	130	0.6	26%	19.3
0.75	130	0.5	25%	19.1
0.75	130	0.7	50%	18.8
0.75	130	0.6	50%	18.6
0.75	120	0.7	50%	18.1

0.10 MPa Pressure

Foam Density (g/cc)	Compr. Temp (°C)	Constraint Diameter (inches)	Percent Compression	60% time (min)
0.25	120	0.5	51%	33.7
0.25	150	0.5	51%	28.6
0.25	120	0.6	50%	23.6
0.50	150	0.6	51%	23.5
0.75	150	0.6	50%	22.6
0.75	140	0.7	51%	21.7
0.50	150	0.5	48%	21.1
0.50	140	0.6	50%	20.9
0.50	140	0.5	48%	20.7
0.50	140	0.7	51%	20.7
0.75	140	0.6	52%	20.6
0.50	120	0.6	51%	20.4
0.50	130	0.6	51%	20.3
0.50	130	0.7	51%	20.3
0.50	130	0.5	47%	19.9
0.50	120	0.5	46%	19.8
0.50	130	0.6	27%	19.5
0.75	130	0.7	50%	19.3
0.50	130	0.5	24%	19.1
0.75	120	0.6	50%	18.9
0.75	130	0.5	24%	18.9
0.75	130	0.6	27%	18.8
0.75	130	0.6	50%	18.7
0.75	120	0.7	50%	18.3

0.13 MPa Pressure

Foam Density (g/cc)	Compr. Temp (°C)	Constraint Diameter (inches)	Percent Compression	60% time (min)
0.50	150	0.6	52%	23.7
0.75	140	0.7	52%	23.0
0.75	150	0.6	50%	22.7
0.50	140	0.5	49%	21.6
0.50	140	0.7	51%	21.5
0.75	140	0.6	51%	21.5
0.50	140	0.6	51%	21.0
0.50	150	0.5	48%	20.6
0.50	120	0.5	48%	20.6
0.50	130	0.6	51%	20.4
0.50	130	0.7	51%	20.3
0.50	130	0.6	28%	20.2
0.50	130	0.5	47%	20.1
0.50	130	0.5	25%	19.9
0.50	120	0.6	50%	19.4
0.75	130	0.6	50%	19.2
0.75	130	0.6	26%	19.1
0.75	120	0.6	51%	18.9
0.75	130	0.5	23%	18.8
0.75	130	0.7	50%	18.8
0.75	120	0.7	50%	18.2

Figure 9 Color-formatted spreadsheets showing 60% recovery times and parameter effects (constraint diameters are shown in inches for simplicity). [Color figure can be viewed in the online issue, which is available at www.interscience.wiley.com.]

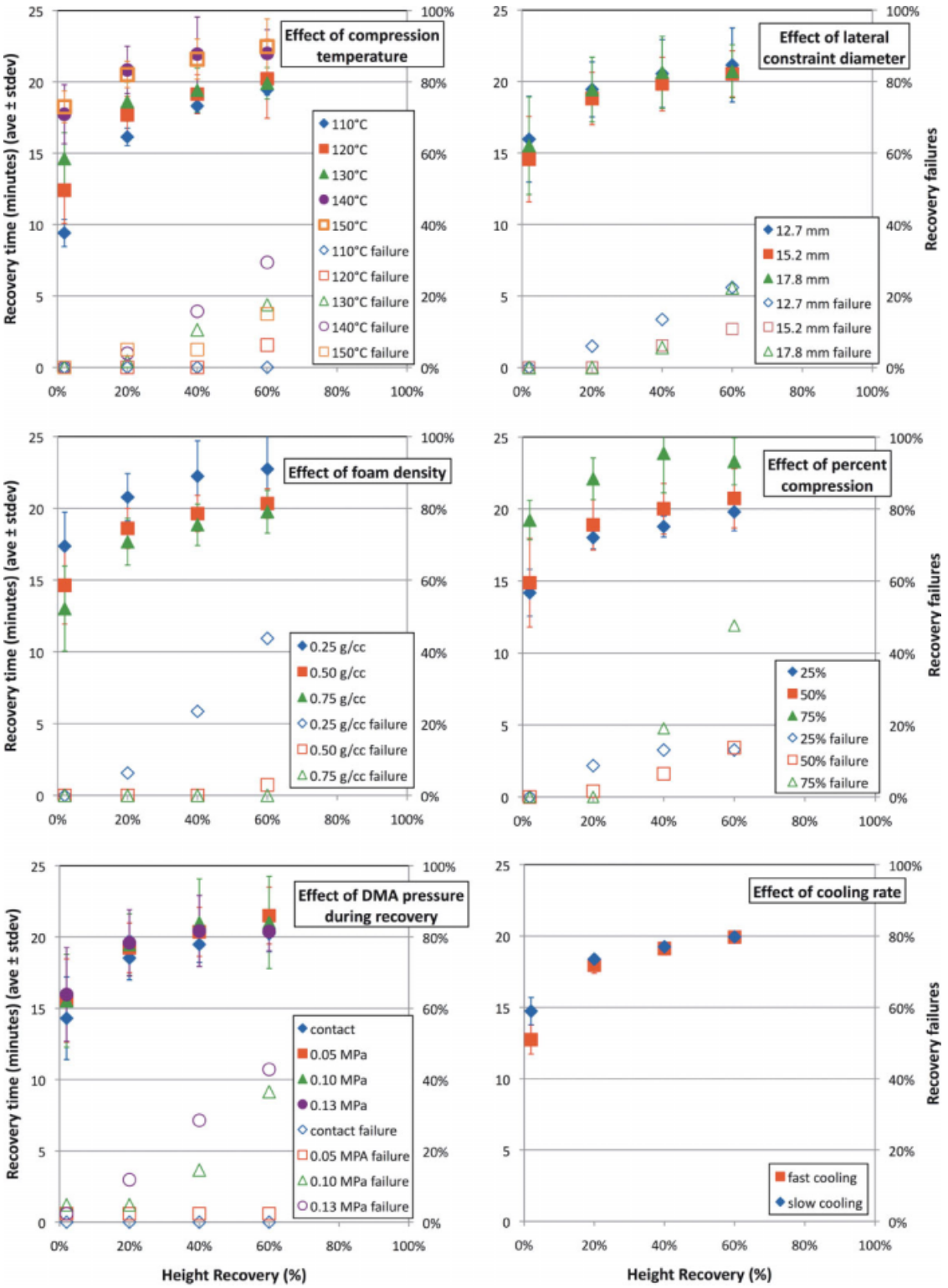

Figure 10 Plots of the effect of each of six parameters on the SMP foam recovery times (left axis) and recovery failure percentages (right axis). [Color figure can be viewed in the online issue, which is available at www.interscience.wiley.com.]

them according to the pressure applied during the DMA run. The actual differences in recovery speed for different parameter combinations are shown and were minimal in many cases. Subtrends, such as the recovery behavior of 0.50 g/cc foams discussed later, could be extracted from such spreadsheets by the selection of particular parameter combinations. Those samples that did not recover to 60% are not

TABLE IV
Height Change in the Compressed Foam Cylinders Stored at Room Temperature

Compression temperature	Average height change (%)	Standard deviation (%)	Number of samples measured	Storage period (days)	Sample parameters (foam density, % compression)
110°C	6.0	±4.7	17	96	0.50 g/cc, 50%
120°C	2.1	±5.0	43	88–96	0.25 g/cc, 50% 0.50 g/cc, 50% 0.75 g/cc, 50%
130°C	−0.2	±4.0	73	154–172	0.25 g/cc, 25, 50, 75% 0.50 g/cc, 25, 50% 0.75 g/cc, 25, 50%
140°C	−2.1	±3.4	80	161–179	0.25 g/cc, 25, 50, 75% 0.50 g/cc, 25, 50% 0.75 g/cc, 25, 50%
150°C	−1.3	±4.1	103	159–180	0.25 g/cc, 25, 50, 75% 0.50 g/cc, 25, 50% 0.75 g/cc, 25, 50%

shown, to account for the decreasing number of samples, particularly, the 0.25 g/cc foams at 0.10 and 0.13 MPa of pressure. These more detailed spreadsheets confirmed the trends noted previously. The changes in the recovery speed with different parameters were generally larger as the recovery speed slowed; this is shown at the top portion of the spreadsheets.

Alternatively, plots of averaged data sorted only by a single parameter also enabled the significance of each parameter to be observed, as shown in Figure 10. The standard deviations were often large in these cases but still showed consistent trends. These plots also show the percentage of each data set (open symbols) that failed to recover to a given level (2–60%). These were the recovery failure values, shown in the right axis. Some of these samples, as noted in the spreadsheet discussion previously, showed recompression, particularly, the low-density, 0.25 g/cc foams, under higher DMA recovery pressures.

Three plots in Figure 10 show little change in recovery time with different parameter values. These include the plots for lateral constraint diameter (top right), DMA pressure during recovery (bottom left), and cooling rate (bottom right, discussed further later). Plots for the compression temperature (top left, discussed further later), foam density (middle left), and percentage compression (middle right) did show changes in recovery times. These same parameters were notable in the spreadsheet comparisons discussed previously.

The compression temperature plot in Figure 10 (top left) includes compressions at temperatures from 110 to 150°C. Only a limited number of compressions were carried out at 110°C on 0.50 g/cc foams compressed 50%, the data for which is not shown in the spreadsheet in Figure 8. Although both the spreadsheet and plot show a clear effect of the compression temperature on the recovery time, the plotted data more clearly demonstrate the magnitude of this effect at different recovery stages.

Lower compression temperatures had a strong effect on the onset of recovery (time to 2% recovery) but had decreasing effects on the time to 20, 40, and 60% recovery. The lack of improvement in the 40–60% recoveries suggested that compression temperatures below the T_g may have, on balance, been undesirable because of their effect on the SMP stability. Slight effects on the foam compression stability were even noticed during storage at room temperature. Although standard deviations of these height measurements were high because of machining variances, Table IV shows higher levels of re-expansion in the samples compressed at 110–120°C. The samples compressed at higher temperatures and also stored for longer periods of time actually showed, on average, slight shrinkage rather than re-expansion. A sharper and higher temperature recovery onset should mitigate premature stress and strain relaxation, even more noticeably when sample storage temperatures are closer to the T_g.

Closer examination of the data for the 0.50 g/cc foams compressed 50%, an attractive system for actuator applications, revealed that the samples compressed above T_g did show noticeable effects on the recovery time of the lateral constraint during compression and the DMA pressure during recovery. The samples compressed at the highest temperature, 150°C, in 15.2 or 17.8 mm (0.6 or 0.7 in.) diameter cavities had longer 60% recovery times, about 22–24 min, than the samples compressed in the smallest diameter (12.7 mm, 0.5 in.) cavities, about 21 min. The samples compressed at 140°C showed much less sensitivity to both the constraint diameter and recovery pressure and had recovery times of about 21 min. The samples compressed at T_g or lower temperatures were affected little by the lateral constraint diameter.

TABLE V
Recovery Times at Different DMA Heating Rates (0.5 g/cc Foams Compressed 50% at 130°C with a DMA Pressure of 0.10 MPa)

DMA heating rate	Time from 60 to 160°C (min)	Time to a specific percentage recovery (min)			
		2%	20%	40%	60%
Maximum[a]	4.3	5.2	6.9	7.8	9.2
20°C/min[a]	6.7	8.6	10.3	11.1	12.2
5°C/min	20.0	14.8	18.6	19.4	20.2

[a] Heating started at 30°C instead of 60°C as in the 5°C/min runs. The heating time from 60 to 160°C at 20°C/min was longer than 5 min because of slowing as the temperature approached 160°C.

All but a limited number of foam compressions in the Carver press were carried out with active water cooling applied immediately after compression. This gave an effective cooling rate of about 4–7°C/min. Temperatures were measured by a thermocouple inserted in one of the foam samples within the compression block. The effect of longer cooling times was evaluated in 0.50 g/cc foams compressed 50% at 120°C in either 12.7 or 15.2 mm diameter cavities. Water-cooled samples reached 100°C in about 5 min. With passive cooling, the sample required about 41 min to reach 100°C, and this allowed more time for stress and strain relaxation. As shown in the cooling plot in Figure 10 (bottom right), only a minor effect was observed on the time to 2% recovery, the onset, whereas no effect was observed on the times to 40 and 60% recovery. The very rapid stress relaxations discussed previously for the test frame experiments indicated that only an extremely rapid cooling rate significantly decreased the amount of stress relaxation, which was consistent with these results.

Times to 20–60% recovery for most of the samples tested, which encompassed a wide range of parameter sets, were typically around 18–20 min. Faster recoveries were evaluated with 0.5 g/cc foams

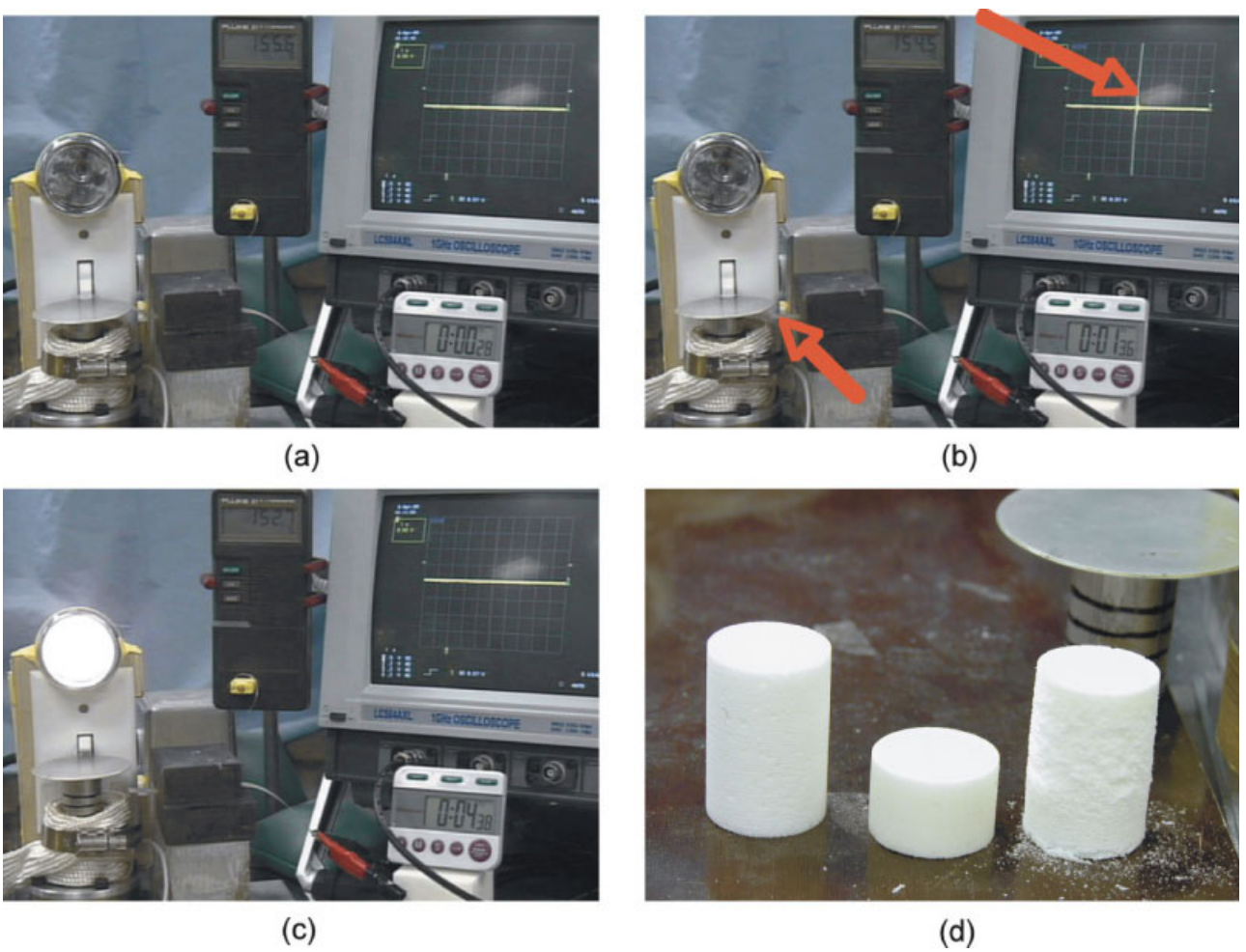

Figure 11 Demonstration of the 0.5-g/cc foam actuator by the (a) heating of a foam cylinder with a metal plunger cap in a cylinder at about 160°C, (b) flipping of a piezoelectric strip to generate an electrical signal of about 4 V, and (c) flipping of a switch to turn on a light bulb. (d) Foam samples as fabricated, compressed, and after recovery. A small amount of surface flaking was evident. [Color figure can be viewed in the online issue, which is available at www.interscience.wiley.com.]

compressed 50% at 130°C and a DMA pressure of 0.10 MPa. We increased the DMA heating rate from 5 to 20°C/min or even higher by simply programming the DMA to immediately equilibrate at 160°C. In these cases, we started the recovery at about 30°C instead of pre-equilibrating at 60°C as in the other DMA runs. As shown in Table V, the recovery times were roughly cut in half.

As an example of an actuator application, a 25 × 38 mm^2 cylinder of a 0.5 g/cc foam was compressed 50% at 130°C and then placed in an aluminum cylinder preheated to 160°C. This apparatus is shown in Figure 11. On expansion, an aluminum plunger placed on top of the expanding foam tripped a piezoelectric strip (held between blocks to the right of the heated cylinder); this generated an electrical signal at about 1.5 min and also flipped a light switch at about 4.5 min. Figure 11(d) shows samples of the foam before compression, after compression, and after recovery in the demonstration.

CONCLUSIONS

The recovery performance of closed-cell urethane SMP foams was evaluated. The compression temperature and foam density had the strongest effects on performance, whereas other parameters had limited effects.

Urethane foam cylinders ranging in density from about 0.25 to 0.75 g/cc were compressed in a range of temperatures to strains of about 25–75%. Different lateral constraints were imposed during compression, and the cooling rates after compression were also varied. Upon reheating, the recovery stresses were measured against fixed platens, whereas the recovery strains were measured against pressures up to 0.13 MPa.

Higher foam densities gave higher recovery stresses, up to 4 MPa for a 0.67 g/cc foam, and also faster strain recoveries. The foam densities evaluated and the recovery stresses measured in these closed-cell foams were higher than those previously reported in the literature. Moderate-density foams ($\sim$ 0.5 g/cc) were most suited for actuator functions and had recovery stresses of 2 MPa or higher. Even lower density foams ($\sim$ 0.25 g/cc) had recovery stresses of about 1 MPa.

The diameters of the foam cylinders were evaluated in a limited sample set with lower density foams and showed no consistent effect on the recovery speed with either 3 or 10°C/min heating rates. It is likely that sample shape and size will affect recovery speed in many circumstances, however. Sample sizes were standardized in this study so that we could evaluate other parameters.

Lateral constraint during compression did not lead to faster recovery rates except in compressions above T_g. Samples compressed at those temperatures, however, had slower recoveries, even with tighter constraints, and such conditions did not provide optimal performance.

The cooling rate after compression, within the range evaluated, had little effect on the strain-recovery rates but did affect the temperature at which recovery began. The absence of stronger effects was attributed to the very rapid stress relaxation that occurred after compression. Much of the compressive stress was lost during this relaxation and limited the subsequent recovery stress. Cooling would need to be nearly instantaneous to retain high levels of the compressive stress.

Compression strain was not an independent parameter, in that higher density foams could not be compressed to the same strains as lower density foams. High compression strains in the 0.25 g/cc foam led to slower recoveries, however. Low compression strains, such as 25%, reduced the height change in the foam available for actuator functions, and moderate strains of about 50% appeared to offer the best balance of performance.

Imposed pressures during recovery, up to 0.13 MPa (19 psi), had surprisingly little effect on the recovery speed, except in the 0.25 g/cc density foams. In some cases, these foams actually recompressed during the DMA recovery runs.

Low compression temperatures, below T_g, caused recovery to begin at lower temperatures but had only modest effects on the recovery time to 40–60% recovery and gave little improvement in the recovery stress. The earlier onset of recovery might also have resulted in the premature relaxation of the SMP foam when it was stored or heated to temperatures near T_g. High compression temperatures, above T_g, gave slower recoveries and lower recovery stresses. Compression near the T_g onset appeared to provide optimal recovery performance.

These results clearly demonstrate the ability of SMP foams, particularly at higher densities, to perform significant levels of mechanical work and actuation.

Many useful discussions were held with Jonathan Zimmerman (Sandia National Laboratories) and T. D. Nguyen (formerly at Sandia and now at Johns Hopkins University). Technical assistance from Roger Watson and Patrick Keifer is gratefully acknowledged. Sandia is a multiprogram laboratory operated by Sandia Corp., a Lockheed Martin Co., for the U.S. Department of Energy under contract DE-AC04-94AL85000.

References

1. Bobovitch, A. L.; Unigovski, Y.; Gutman, E. M.; Kolmakov, E.; Vyazovkin, E. S. J Appl Polym Sci 2007, 103, 3718.
2. Trznadel, M.; Kryszewski, M. J Macromol Sci Rev Macromol Chem Phys 1992, 32, 259.

3. Arzberger, S. C.; et al. Proc SPIE-Int Soc Opt Eng 2005, 5762, 35.
4. Baer, G.; Wilson, T. S.; Mathews, D. L.; Maitland, D. J. J Appl Polym Sci 2007, 103, 3882.
5. Gall, K.; Yakacki, C. M.; Liu, Y.; Shandas, R.; Willett, N.; Anseth, K. S. J Biomed Mater Res A 2005, 73, 339.
6. Lu, X. L.; Sun, Z. J.; Cai, W.; Gao, Z. Y. J Mater Sci Mater Med 2008, 19, 395.
7. Sokolowski, W. Proc SPIE-Int Soc Opt Eng 2005, 5648, 397.
8. Yakacki, C. M.; Shandas, R.; Lanning, C.; Rech, B.; Eckstein, A.; Gall, K. Biomaterials 2007, 28, 2255.
9. Chen, S.; Hu, J.; Zhuo, H.; Zhu, Y. Mater Lett 2008, 62, 4088.
10. Behl, M.; Lendlein, A. Mater Today 2007, 10, 20.
11. Ratna, D.; Karger-Kocsis, J. J Mater Sci 2008, 43, 254.
12. Liu, C.; Qin, H.; Mather, P. T. J Mater Chem 2007, 17, 1543.
13. Beloshenko, V. A.; Varyukhin, V. N.; Voznyak, Y. V. Russ Chem Rev 2005, 74, 265.
14. Lendlein, A.; Kelch, S. Angew Chem Int Ed 2002, 41, 2034.
15. Nguyen, T. D.; Qi, H. J.; Castro, F.; Long, K. N. J. Mech Phys Solids 2008, 56, 2792.
16. Chen, Y. C.; Lagoudas, D. C. J. Mech Phys Solids 2008, 56, 1752.
17. Chen, Y. C.; Lagoudas, D. C. J. Mech Phys Solids 2008, 56, 1766.
18. Qi, H. J.; Nguyen, T. D.; Castro, F.; Yakacki, C. M.; Shandas, R. J. Mech Phys Solids 2008, 56, 1730.
19. Liu, Y.; Gall, K.; Dunn, M. L.; Greenberg, A. R.; Diani, J. Int J Plasticity 2006, 22, 279.
20. Liu, Y.; Gall, K.; Dunn, M. L.; McCluskey, P. Smart Mater Struct 2003, 12, 947.
21. Yakacki, C. M.; Willis, S.; Luders, C.; Gall, K. Adv Eng Mater 2008, 10, 112.
22. Tey, S. J.; Huang, W. M.; Sokolowski, W. M. Smart Mater Struct 2001, 10, 321.
23. Di Prima, M. A.; Lesniewski, M.; Gall, K.; McDowell, D. L.; Sanderson, T.; Campbell, D. Smart Mater Struct 2007, 16, 2330.
24. Huang, W. M.; Lee, C. W.; Teo, H. P. J. Intelligent Mater Syst Struct 2006, 17, 753.
25. Tobushi, H.; Okumura, K.; Endo, M.; Hayashi, S. J. Intelligent Mater Syst Struct 2001, 12, 283.
26. Tobushi, H.; Shimada, D.; Hayashi, S.; Endo, M. Proc Inst Eng 2003, 217(Part L), 135.
27. Tobushi, H.; Matsui, R.; Hayashi, S.; Shimada, D. Smart Mater Struct 2004, 13, 881.
28. Tobushi, H.; Hayashi, S.; Hoshio, K.; Miwa, N. Smart Mater Struct 2006, 15, 1033.
29. Tobushi, H.; Hayashi, S.; Hoshio, K.; Ejiri, Y. Sci Technol Adv Mater 2008, 9, 1.
30. Wilson, T. S.; Bearinger, J. P.; Herberg, J. L.; Marion, J. E.; Wright, W. J.; Evans, C. L.; Maitland, D. J. J Appl Polym Sci 2007, 106, 540.
31. Ping, P.; Wang, W.; Chen, X.; Jing, X. J Polym Sci Part B: Polym Phys 2007, 45, 557.
32. Ji, F. L.; Zhu, Y.; Hu, J. L.; Liu, Y.; Yeung, L. Y.; Ye, G. D. Smart Mater Struct 2006, 15, 1547.